170–180 *Nucleic Acids Research, 2012, Vol. 40, No. 1* *Published online 9 September 2011*
doi:10.1093/nar/gkr596

DNA damage bypass operates in the S and G2 phases of the cell cycle and exhibits differential mutagenicity

Noam Diamant[1], Ayal Hendel[1], Ilan Vered[1], Thomas Carell[2], Thomas Reißner[2], Niels de Wind[3], Nicholas Geacinov[4] and Zvi Livneh[1,*]

[1]Department of Biological Chemistry, Weizmann Institute of Science, Rehovot 76100, Israel, [2]Department of Chemistry and Biochemistry, Ludwig-Maximilians-University Munich, 81377 München, Germany, [3]Department of Toxicogenetics, Leiden University Medical Center, PO Box 9600, 2300 RC Leiden, The Netherlands and [4]Department of Chemistry, New York University, New York, NY 10003-5180, USA

Received February 27, 2011; Revised June 16, 2011; Accepted July 5, 2011

ABSTRACT

Translesion DNA synthesis (TLS) employs low-fidelity DNA polymerases to bypass replication-blocking lesions, and being associated with chromosomal replication was presumed to occur in the S phase of the cell cycle. Using immuno-staining with anti-replication protein A antibodies, we show that in UV-irradiated mammalian cells, chromosomal single-stranded gaps formed in S phase during replication persist into the G2 phase of the cell cycle, where their repair is completed depending on DNA polymerase ζ and Rev1. Analysis of TLS using a high-resolution gapped-plasmid assay system in cell populations enriched by centrifugal elutriation for specific cell cycle phases showed that TLS operates both in S and G2. Moreover, the mutagenic specificity of TLS in G2 was different from S, and in some cases overall mutation frequency was higher. These results suggest that TLS repair of single-stranded gaps caused by DNA lesions can lag behind chromosomal replication, is separable from it, and occurs both in the S and G2 phases of the cell cycle. Such a mechanism may function to maintain efficient replication, which can progress despite the presence of DNA lesions, with TLS lagging behind and patching regions of discontinuity.

INTRODUCTION

Translesion DNA synthesis (TLS) is a DNA damage tolerance mechanism that assists replication to overcome blocking lesions. It is inherently mutagenic due to the miscoding nature of most DNA lesions, and the promiscuous active site of the TLS DNA polymerases involved in the process (1–4). Despite its inherent mutagenic nature, TLS has a major role in protecting humans against DNA damage, as indicated by the high sunlight sensitivity and skin cancer pre-disposition of individuals with germ-line mutations, which inactivate the TLS DNA polymerase (pol) η (5,6). Mammalian cells contain multiple TLS polymerases (7), which exhibit a certain degree of DNA damage specificity and act largely via two-polymerase mechanisms in which insertion opposite the lesion is carried out by one polymerase, and extension past the lesion by a second polymerase, usually polζ (2,8–10). The DNA sequence resulting from TLS is largely determined by the inserter DNA polymerase (2,8). TLS is tightly regulated at several levels to prevent an escalation in mutation rates. This includes monoubiquitination of proliferating cell nuclear antigen (PCNA), which is induced by DNA damaging agents and serves to recruit TLS polymerases to the damaged site in DNA (11–13), as well as the p53 and p21 proteins, which restrain TLS and make it more accurate (14).

TLS was believed to be associated with DNA replication, and therefore, to occur in the S phase of the cell cycle (15). However, it was shown that DNA replication skips template regions containing lesions formed by damaging agents such as ultraviolet (UV) radiation, leaving behind single-stranded DNA (ssDNA) gaps (16–19). The repair of these gaps was termed post-replication repair, suggesting that it occurs behind the replication fork. However, to which extent does TLS lag behind replication forks, and whether it is confined to the S phase of the cell cycle was largely unexplored. Recently, studies from two labs demonstrated that TLS can occur in the G2 phase of the cell cycle in the yeast *Saccharomyces cerevisiae*, suggesting that TLS is separable from chromosomal replication (20,21). Here, we describe our study of the operation of TLS along the various cell cycle phases in mammalian

*To whom correspondence should be addressed. Tel: +972 8 934 3203; Fax: +972 8 934 4169; Email: zvi.livneh@weizmann.ac.il

cells. We found that in human and mouse cells, TLS is as high or higher in G2 compared to S phase, indicating that it lags behind chromosomal replication. Moreover, the mutagenic signature in G2 was different than in S, and the overall mutation frequency was higher for some lesions.

MATERIALS AND METHODS

Cell lines, DNA constructs and antibodies

The U2OS cell line was derived from human osteosarcoma. Wild-type mouse embryonic fibroblasts (MEF) were previously described (18). Cells were maintained in Dulbecco's Modified Eagle's Medium (DMEM) supplemented with 2 mM glutamine. The medium was supplemented with 10% fetal bovine serum, 100 U/ml of penicillin and 100 μg/ml streptomycin. Cells were incubated at 37°C in a 5% CO_2 atmosphere. The construction of gapped plasmids carrying site-specific TT CPD, TT 6-4PP, cisPt-GG or BP-G was previously described (8,22). Sources of antibodies were as follows: mouse monoclonal anti-polη antibody (B-7): sc-17770 (used at a dilution of 1:200 in western blot, Santa Cruz Biotechnology); rabbit polyclonal anti-pol Iota NB100-175 (used at a dilution of 1:500 in western blot, Novus Biologicals); anti-Rev1 Rabbit polyclonal (used at a dilution of 1:500 in western blot, a generous gift from Sam H. Wilson, NIEHS, NC, USA) (23); rabbit polyclonal anti-cyclinA (H-432):sc-751 (used at a dilution of 1:1000 in western blot, Santa Cruz Biotechnology); mouse anti-replication protein A (RPA)-32/RPA-2 [used at a dilution of 1:500 for immuno-flouresence, AbCam (cat. no: ab2175)]; mouse monoclonal anti-PCNA, PC-10 (used at a dilution of 1:1000 in western blot, Sigma); mouse anti-tubulin, (DM1A, Sigma); anti-p21 antibody (F5 or C19, Santa Cruz Biotechnology); Rabbit polyclonal anti γ-Tubulin (ab11317, used at a dilution of 1:2000 for immuno-flouresence, Abcam).

Fractionation of cells in the G1, S and G2 phases of the cell cycle

Human U2OS cells or mouse embryo fibroblasts were fractionated by centrifugal elutriation as described (24), using a J6 Beckman elutriation centrifuge with a JE-5.0 rotor equipped with a single-standard 5 ml elutriation chamber (Beckman Coulter, Inc., Fullerton, CA, USA) and a masterflex microprocessor pump drive, model 7524-05 (Cole Parmer).

Analysis of RPA foci by fluorescence microscopy

For RPA immunostaining, cells were seeded on 13-mm glass cover slips coated with 0.01% poly-L-lysine (Sigma). After 90 min of the cells attaching to the slides, the medium was removed and the cells were UV-irradiated at 254 nm using a low-pressure mercury lamp at doses of 1–10 J/m^2. The dose rate was determined by a UV-products radiometer using a UVX-25 sensor. At various time points, cells were washed three times with PBS, pre-extracted in 25 mM HEPES pH 7.4, 50 mM NaCl, 3 mM $MgCl_2$, 300 mM sucrose, 0.5% Triton X-100 for 5 min on ice with gentle shaking and washed three more times with PBS. The slides were then fixed with 4% paraformaldehyde for 15 min at room temperature, and washed three times in PBS. Blocking was done in PBS supplemented with 5% normal goat serum (Sigma) for 30 min at room temperature. The cells were incubated for 1 h with anti-RPA32 mouse antibodies at a dilution of 1:500, and anti γ-tubulin rabbit antibodies at a dilution of 1:1000. After the incubation, the slides were washed three times in PBS and incubated with a secondary goat anti-mouse Alexa Fluor 488 (green) antibody (Jackson, diluted 1:1000) and goat anti-rabbit cy3 (Jacskon,1:2000) and with 4′,6-diamidino-2-phenylindole (DAPI) diluted 1:1000 for 45 min. The slides were then washed three times in PBS and mounted on microscope slides using Prolong gold reagent (Invitrogen). Images were captured with a DeltaVision system (Applied Precision) equipped with an Olympus IX71 microscope. Optical images were acquired using CCD camera (Photometrics, Coolsnap HQ) and a ×60/1.42 objective (Olympus). To determine the fraction of RPA positive cells, the number of cells in each field was counted by the DAPI stain and then the filter was changed and RPA positive cells were counted. In each sample, at least 10 fields and 100 cells were scored. Similarly, in order to determine the cell cycle state of RPA positive cells. The RPA positive cells in each field were counted and then the filter changed, and the centrosome state in each cell was determined by γ-tubulin staining. In experiments with siRNA treatment, U2OS cells were transfected with 10 nM siRNA oligos (Darmacon, siGENOME) in 15 cm plates, at 30% confluence. After 48 h, the cells were split to new plates, and after 24 additional h (total of 72 h with siRNA), the cells were synchronized by centrifugal elutriation, UV-irradiated and then analyzed for RPA foci and cell cycle progression.

TLS assay in elutriation-fractionated cells

The TLS assay was done as previously described (8,14,22) with some minor changes. In each transfection, $1–1.5 \times 10^6$ U2OS or MEF cells were electroporated using Amaxa Nucleofector® Device (Lonza, Switzerland). The transfected DNA was a mixture composed of the following: 100–200 ng of a gapped-lesion plasmid (bearing a kan^R cassette), 100–200 ng of a gapped plasmid without lesion (bearing a cm^R cassette) and 5 μg of the carrier plasmid pUC18. After the incubation time (indicated separately for each experiment), the cells were harvested and plasmid DNA was extracted using a plasmid extraction kit (RBC biosciences, Taiwan). The DNA was transformed into a TLS-deficient *Escherichia coli recA* strain by electroporation and plated on LB plates containing either kanamycin or chloramphenicol. The percentage of lesion–plasmid survival was calculated by dividing the number of transformants obtained from the gap-lesion plasmid (number of colonies on LB-kan plates) by the number of corresponding transformants obtained with the control gapped plasmid GP20-cm (number of colonies on LB-cm plates). Plasmids were extracted from kan^R colonies, and the sequence opposite the lesion was determined using Bigdye Terminator V1.1

Cycle sequencing (Applied Biosystems,USA) and analyzed using 3130XL genetic analyzer (Applied Biosystems, USA). To obtain values of TLS from values of gap repair, the latter were multiplied by the percentage of TLS events out of the total events, as determined by the DNA sequence analysis.

RESULTS

RPA foci are formed in the S phase in UV-irradiated human cells

Seeking to determine the activity of TLS during the cell cycle, we analyzed the formation and disappearance of ssDNA regions in UV-irradiated human cells during chromosomal replication. Such regions represent replication forks arrested at sites of UV damage, and gaps whereby replication skipped over UV damage [post-replication gaps; reviewed in (25)]. To measure these ssDNA regions, we used immunofluorescence staining of RPA foci (26). RPA is a trimeric protein that specifically binds ssDNA, and is essential for DNA replication as well as other DNA transactions (27). As can be seen in Figure 1A, staining of RPA in the nuclei of unirradiated human U2OS cells was scarce. In contrast, after UV irradiation at $10\,J/m^2$, the majority of nuclei exhibited robust formation of RPA foci (Figure 1A). To concentrate on gaps formed by UV during replication, we used the UV-irradiated cells that were enriched for the G1/S boundary stage by centrifugal elutriation, using cells in the G1 phase as a control. The advantage of centrifugal elutriation for isolating cells at the various cell cycle stages is that it does not involve any drugs, and therefore likely to be free of any interfering effects.

U2OS cells were fractionated by centrifugal elutriation, and fractions at G1 or at the G1/S boundary were UV-irradiated at $3\,J/m^2$ (43% survival; Supplementary Figure S1A) allowed to grow for 2 h, and then fixed and immunostrained for RPA. As can be seen in Figure 1B, unirradiated cells contained a low background of RPA foci, as expected, since the abundance of persisting ssDNA regions in the absence of DNA damage was low. G1-irradiated cells also exhibited a low level of RPA foci, consistent with the lack of replication during this cell cycle stage (Figure 1B). In contrast, when cells were irradiated at the G1/S boundary, the percentage of cells with RPA foci increased compared to cells irradiated at G1 (Figure 1B), suggesting that the staining of RPA reflects ssDNA regions that were formed during S phase.

UV-induced RPA foci formed during S phase disappear primarily in the G2 phase

To follow the fate of UV-induced RPA foci, we irradiated human U2OS cells at the G1/S boundary with a UV dose of $3\,J/m^2$, and then monitored in parallel cell cycle progression and RPA foci for up to 32 h post-irradiation. As can be seen in Figure 1C, UV irradiation at this UV dose caused a delay in cell cycle progression, which recovered by 32 h (Figure 1C). Under these conditions, the number of cells with RPA foci increased for up to 8 h post-irradiation, then declined, reaching the background level by 24 h (Figure 1D). This behavior is consistent with an accumulation of replication gaps, followed by DNA damage tolerance that restored the double-stranded structure. Strikingly, RPA foci disappeared 16–24 h after irradiation, a time period in which most of the cells were in G2 (Figure 1D). To directly examine whether RPA foci exist in cells that are in G2, we performed double staining for RPA and the centrosomic protein γ-tubulin, which can be used as a marker for cells in G2 (28). After verifying that the cell cycle distribution as predicted by γ-tubulin correlates with that reflected in the fluorescence-activated cell sorting (FACS) analysis (Supplementary Figure S1B), we determined the cell cycle distribution of RPA positive cells. As can be seen in Figure 1E, about half of the RPA positive cells were in G2, indicating that a significant fraction of UV-induced gaps were not filled in during S and entered G2, where they were later filled in. Repeating the experiment with cells irradiated at $10\,J/m^2$ revealed a severe arrest at G2, massive cell death (Supplementary Figure S1C) and persistence of RPA foci (Supplementary Figure S1D).

Disappearance of RPA foci is dependent on the TLS DNA polymerase ζ and Rev1

To examine whether the disappearance of RPA foci in U2OS cells had occurred by TLS, we knocked down the expression of the *REV3L* gene encoding the catalytic subunit of DNA polymerase ζ (Supplementary Figure S2D), and followed the formation and disappearance of RPA foci after UV irradiation. As can be seen in Figure 2A, UV irradiation of the cells at the G1/S boundary caused a delay in cycle progression, which was more pronounced for cells treated with *REV3*L siRNA compared to control siRNA (Figure 2A). Analysis of RPA foci showed that 12 h after irradiation of cells treated with a control siRNA, RPA foci were abundant, but most of them disappeared by 20 h after irradiation (Figure 2B). In contrast, in cells treated with *REV3L* siRNA, RPA foci persisted also at 20 h after irradiation (Figure 2B). Background levels of RPA foci were observed in unirradiated cells, possibly the result of replication gaps caused by background DNA damage. The quantification of the analysis is shown in Figure 2C. In cells treated with the control siRNA, the number of RPA foci was reduced to background level by 20 h after irradiation, with 6.5% of the cells exhibiting RPA foci. In contrast, when expression of *REV3L* was knocked down, there was a strong inhibition in disappearance of RPA foci, with 37% of the cells still containing RPA foci 20 h after irradiation, >5-fold higher than the control cells (Figure 2C). Performing similar experiments with U2OS cells in which the expression of REV1 was knocked down (Supplementary Figure S2C), showed generally a similar result, although the inhibition in the disappearance of RPA foci was milder (Figure 2D and Supplementary Figure S2). These data indicate that TLS is involved in the disappearance of RPA foci, consistent with a previous report that TLS is the main mechanism for filling in post-replication DNA gaps in mouse cells (18). Moreover, the data show that polζ and REV1 have a major role in the repair of

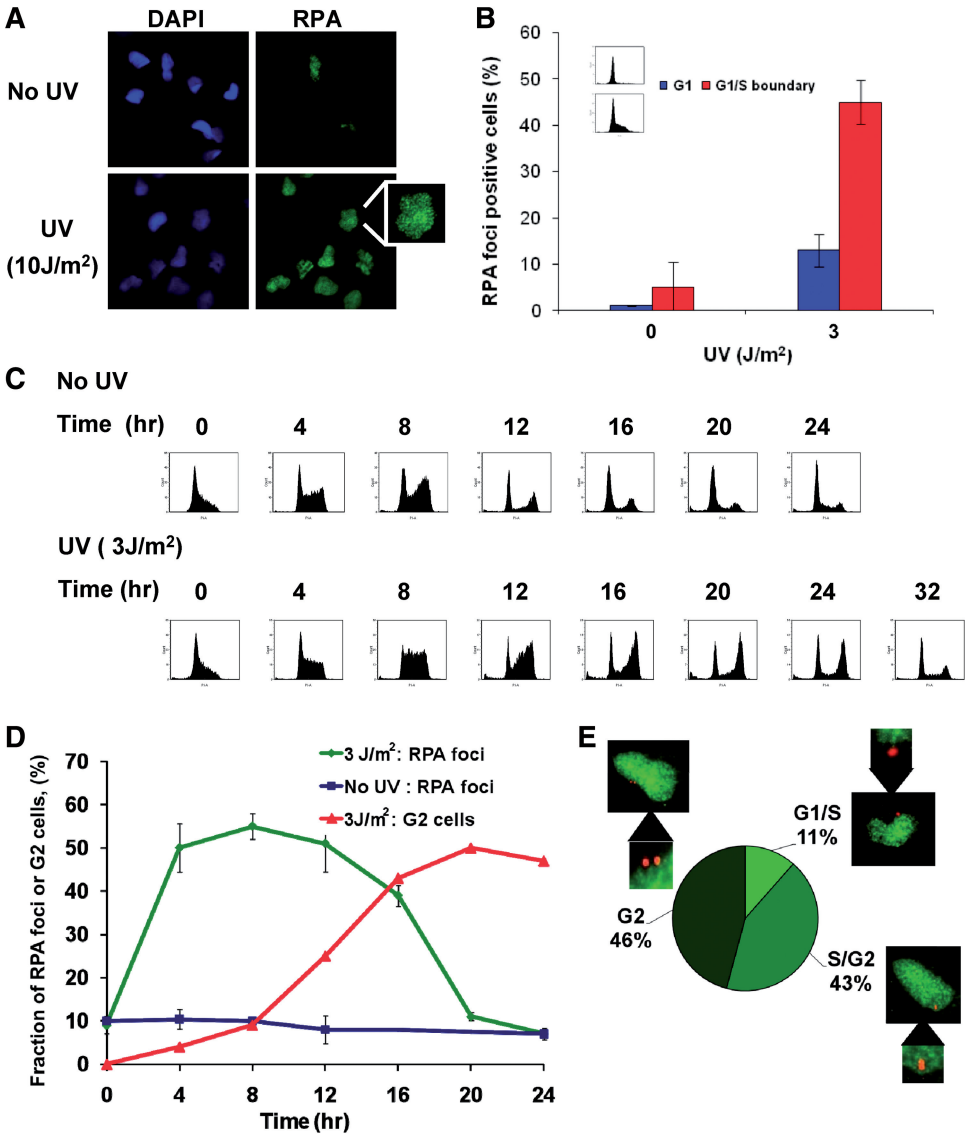

Figure 1. Formation and disappearance of RPA foci following UV irradiation. (**A**) RPA foci. U2OS cells were irradiated at 10 J/m^2 UV, fixed after 2 h and immunostained with anti-RPA antibodies. (**B**) Formation of RPA foci during replication of UV-irradiated cells. U2OS cell populations at G1 and at the G1/S transition were irradiated at 3 J/m^2 UV, fixed after 2 h and immunostained for RPA. In this experiment and all subsequent RPA staining experiments, quantification was done by first detecting cells by DAPI staining and then scoring positive or negative for RPA foci. Approximately 150 cells were scored for each sample. (**C**) Cell cycle profiles of U2OS cells with or without UV irradiation at 3 J/m^2. (**D**) Kinetics of RPA foci formation and clearance after 3 J/m^2 UV treatment. Values of RPA positive cells at each time point are compared with the portion of cells in the G2 phase in the irradiated population. (**E**) Analysis of cell cycle distribution of RPA foci-positive cells 16 h after UV irradiation at 3 J/m^2. Cells were co-stained for RPA (green) and γ-tubulin (red). γ-Tubulin stains the centrosomes, and is used to determine the cell cycle status. G2 cells have fully duplicated and separated centrosomes, which appear as two distinct red dots.

chromosomal ssDNA gaps in human cells, consistent with previous studies carried out with mouse cells (18,29). The ability to follow by RPA staining the repair of chromosomal UV-induced replication gaps adds a significant tool to the currently available DNA damage tolerance assays.

Analysis of the expression of TLS proteins at various cell cycle stages

We analyzed the expression of three TLS polymerases at the various cell cycle stages: polη and polι and Rev1, a TLS regulatory protein with restricted dCMP transferase activity (18,30), which was reported to be highly induced in G2 in *S. cerevisiae* (31). This was done in human U2OS cell fractions enriched by centrifugal elutriation for the G1, S or G2 phases of the cell cycle. As can be seen in Figure 3A, immunoblot analysis showed no significant differences in the amounts of these polymerases at the various cell cycle stages, although there appeared to be a mildly higher amount of polη in G2. Analysis of mRNA expression by real-time polymerase chain reaction (PCR) showed a mild increase in polη mRNA from G1 through S to G2 (Figure 3B), whereas, the levels of Rev1 mRNA were similar (Figure 3C). We have also determined the amount of monoubiquitinated PCNA (Ub-PCNA)

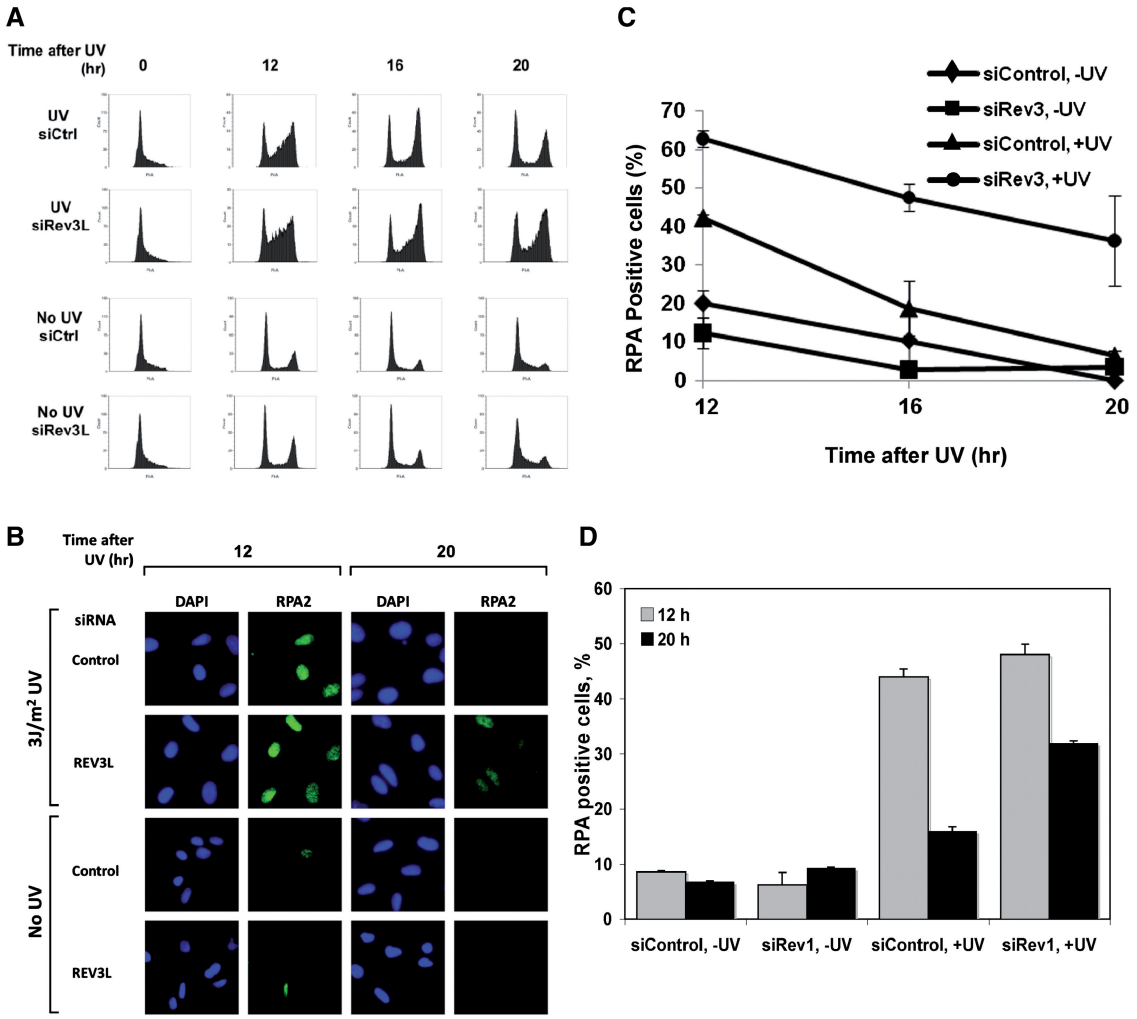

Figure 2. Time course of cell cycle status and RPA foci in UV-irradiated cells in which the expression of DNA polymerase ζ or Rev1 was knocked down. (**A**) Cell cycle profiles of U2OS cells treated with siControl or si*REV3L* (encoding the catalytic subunit of polζ) with or without UV irradiation at 3 J/m^2. (**B**) Representative images of UV-irradiated and unirradiated cells, in which the expression of polζ was knocked down by treatment with *REV3L* siRNA. Staining was done with DAPI (blue) and anti-RPA2 antibodies (green). (**C**) Time course of RPA foci clearance 12–20 h after 3 J/m^2 UV treatment. Unirradiated cells treated with siControl (filled diamond) or si*REV3L* (filled square) were compared to UV-irradiated cells treated with siControl (filled triangle) or si*REV3L* (filled circle). (**D**) RPA foci clearance after 3 J/m^2 UV treatment of U2OS cells that were pre-treated with *REV1* siRNA or control siRNA. See Supplementary Figure S2 for RPA foci images and cell cycle analysis.

(13,32), which enables recruitment of TLS polymerases to DNA following DNA damage. In unirradiated cells ubiquitinated PCNA was undetectable (Figure 3D). In UV-irradiated cells, soluble PCNA was not modified, but chromatin-bound PCNA was monoubiquitinated, as expected. However, the levels of Ub-PCNA appears to be similar in all cell cycle stages (Figure 3D), suggesting that the cell cycle regulation of TLS is not determined by Ub-PCNA *per se*. Ub-PCNA was present also in the G1 phase, suggesting that in UV-irradiated cells, PCNA is monoubiquitinated also in the absence of replication.

TLS is as high or higher in G2 compared to the S phase of the cell cycle

To directly measure TLS during the different phases of the cell cycle, we utilized a quantitative TLS assay based on gapped plasmids carrying a gap opposite a defined and site-specific lesion. This gapped plasmid assay has been extensively used in our laboratory, and proved to be a powerful model for TLS, exhibiting dependence on the polymerase composition of cells and being subject to regulation in a manner similar to that observed in chromosomal TLS (8,14,22,33,34).

The experimental scheme is outlined in Figure 4A. Human U2OS cell fractions enriched for the G1, S or G2 phases of the cell cycle were isolated by centrifugal elutriation, and transfected with a gapped plasmid carrying a site-specific lesion in a single-stranded region, along with a control gapped plasmid with no lesion. Transfection was carried out by electroporation in order to facilitate rapid entry of the plasmids into the cell nucleus. The cells were incubated for 1–1.5 h to allow time for gap filling via TLS to occur, after which the plasmid content was extracted and assayed for TLS.

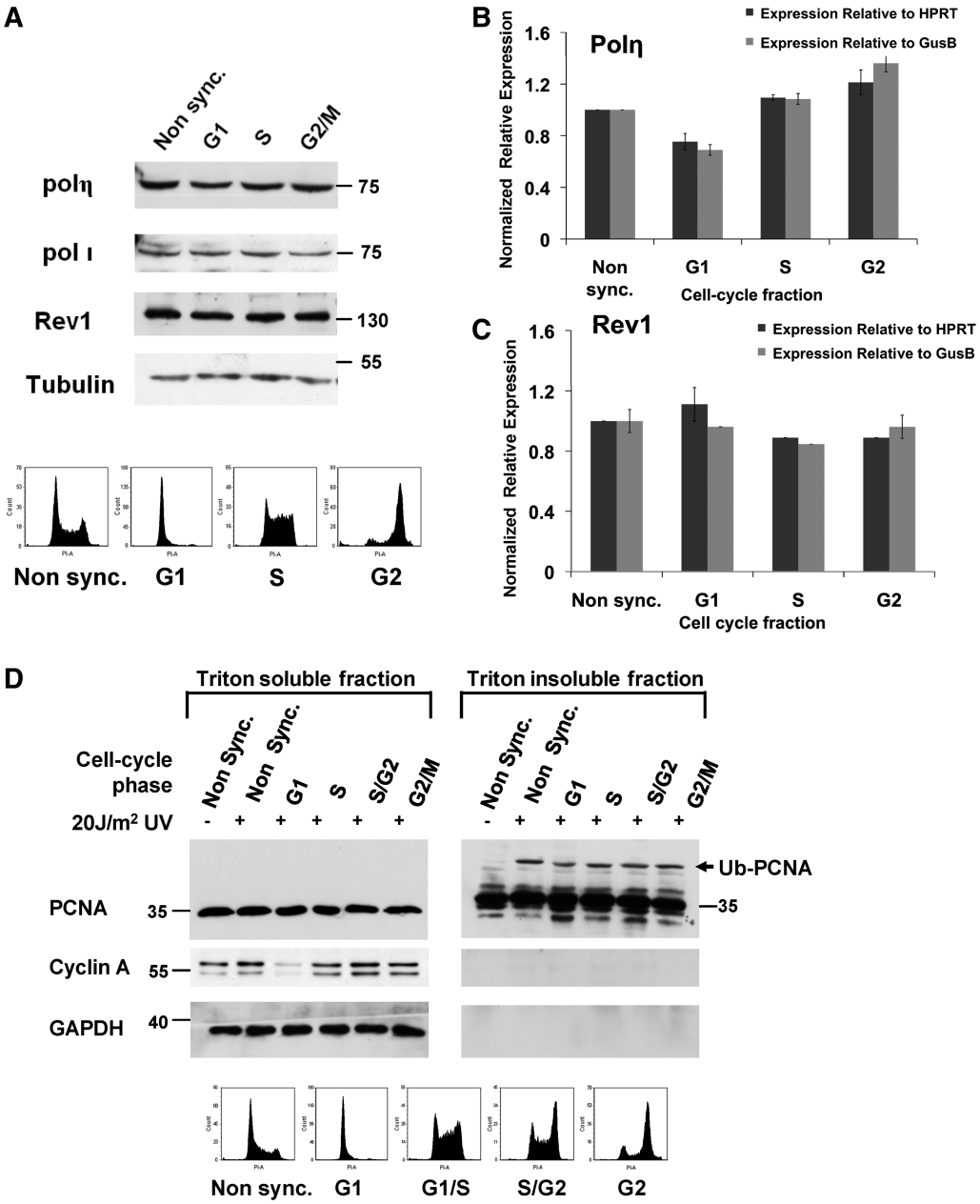

Figure 3. Analysis of cell cycle-dependent expression of TLS polymerases and PCNA ubiquitination. (**A**) U2OS cells were fractionated by centrifugal elutriation to fractions enriched for specific cell cycle phases, and analyzed for expression levels of Polη, Polι and Rev1 using western blot analysis. (**B**) Analysis of polη mRNA levels at different cell cycle stages using real-time PCR. (**C**) Analysis of mRNA levels of Rev1 at different cell cycle stages using real-time PCR. (**D**) Analysis of PCNA monoubiquitination at different cell cycle stages. U2OS cells were separated to fractions enriched for specific cell cycle phases, UV-irradiated ($20\,J/m^2$), and 4 h later soluble (left panel; triton soluble) and chromatin-bound (right panel; triton insoluble) proteins were extracted and analyzed for the extent of PCNA monoubiquitination (Ub-PCNA) using anti-PCNA antibodies.

Importantly, the cell cycle status only minimally changed during this short time window that was used to assay TLS (Figure 4B). Figure 4C and Supplementary Tables S3 and S4 show the results of a TLS experiment performed with a gapped plasmid carrying a site-specific thymine–thymine cyclobutane pyrimidine dimer (TT CPD), the main UV lesion in DNA. TLS in U2OS cells enriched for the S phase was 42%, ~2-fold higher than during G1. When measured in G2, TLS was even higher, amounting to 62%. To examine the situation in another cell type, we used mouse embryo fibroblasts (MEF). We found that in these cells TLS across a TT CPD in G2 was 57%, compared with 34% and 15% in S and G1, respectively (Figure 4C and Supplementary Table S4).

We also tested TLS across another lesion, an intrastrand cisplatin-GG adduct (cisPt-GG), the main DNA lesion caused by the chemotherapy drug cisplatin. As can be seen in Figure 4D and Supplementary Tables S3 and S4, similarly to the bypass of the TT CPD, TLS across cisPt-GG was higher in G2 and S than in G1 in both

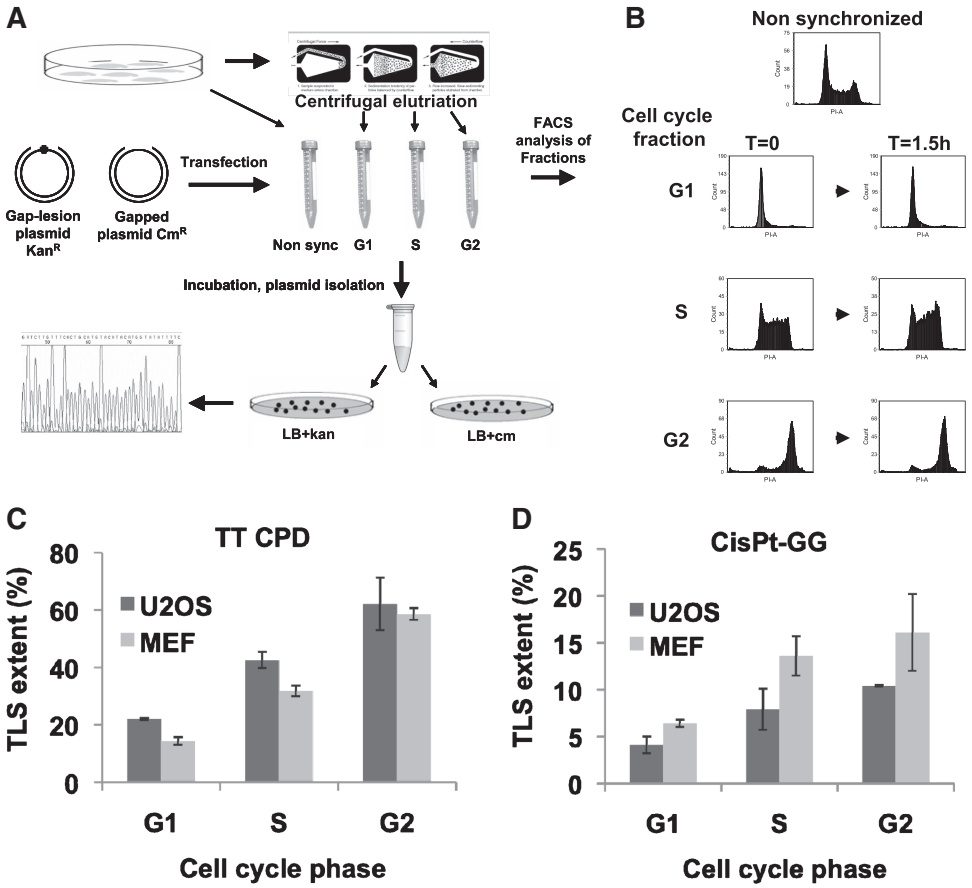

Figure 4. Translesion DNA synthesis in G2 is as high or higher than in S phase. TLS efficiency across DNA lesions in human and murine cell lines was measured using the gapped plasmid assay system. (**A**) A schematic representation of the experimental system. (**B**) A representative sample of the cell cycle fractions that were collected by centrifugal elutriation, and subsequently used for the TLS experiments shown below. Samples that were analyzed by flow cytometry were first mock transfected to mimic the treatment used in the TLS assay. Analysis of TLS was performed at the various cell cycle stages for TT CPD (**C**) and cisPt-GG (**D**). Each graph represents the average of at least three independent experiments. The detailed numerical results are presented in Supplementary Tables S3 and S4.

U2OS human cells and MEF. Interestingly, the TLS machinery appears to remain functional also in the G1 phase.

Different mutagenic signature and lower fidelity of TLS in G2 compared to S

DNA sequence analysis of the plasmids allowed us to determine the accuracy and error spectrum of TLS at the various cell cycle stages. As can be seen in Figure 5A and Supplementary Table S4, TLS across cisPt-GG in MEF was largely accurate, consistent with previous results (8). However, the overall error frequency was not uniform throughout the cell cycle. Thus, out of the TLS events, the error frequency at the cisPt-GG lesion in G2 was 8%, ~3-fold higher than in S (2.8%; $P = 0.032$, χ^2 test). The same analysis in human U2OS cells revealed a similar trend (Figure 5A and Supplementary Table S3).

We analyzed the mutagenic signature of two additional lesions in MEF cells. As can be seen in Figure 5B and Supplementary Table S4, the overall mutagenicity of TLS across a thymine–thymine 6-4 photoproduct (TT 6-4PP), a highly mutagenic UV lesion, was similar at the various cell cycle stages. However, there were differences in the mutagenic signatures (Figure 5B and Supplementary Table S4). Most notable, the $\underline{\text{AAC}}\rightarrow\text{AAA}$ hotspot mutation, a hallmark mutation of $\overline{\text{TT}}$ 6-4PP (34,35), was much more prevalent in G2 (19.4% of all TLS events) compared with S (9.3% of all TLS events; $P = 0.008$, χ^2 test), and G1 (3.7% of all TLS events; $P = 0.00001$, χ^2 test). When studying BP-G [the (+)–*trans*-BPDE N^2-guanine adduct], a major tobacco smoke adduct, overall mutagenic TLS was similar in the various cell cycle stages and accounted for 10–15% of all TLS events (Figure 5C and Supplementary Table S4). However, like in the case of the TT 6-4PP, there was a difference in mutagenic signature at the various cell cycle stages (Figure 5C and Supplementary Table S4) Thus, the C→A mutation opposite the BP-G accounted for 8.5% of all TLS events in G2, but only 1.8% in S ($P = 0.021$, χ^2 test) and <1% in G1 ($P = 0.0045$; χ^2 test).

DISCUSSION

Regions of ssDNA caused by interruption of replication at DNA lesions can be repaired to yield a double-stranded configuration by one of the two known tolerance mechanisms, namely TLS, or homology-dependent repair (HDR), which includes homologous recombination repair (HRR) and template switch recombination (16,36–40). The

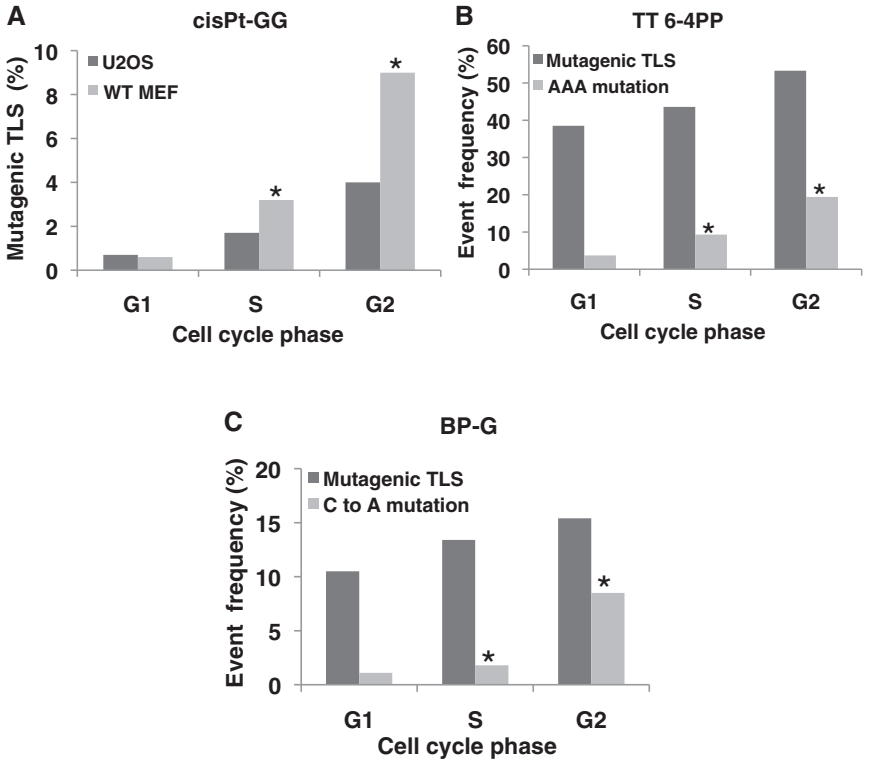

Figure 5. TLS specificity at the various cell cycle phases. TLS experiments were performed in cells enriched for defined stages of the cell cycle using the gapped plasmid assay system as described in the legend to Figure 4, after which plasmids were subjected to DNA sequence analysis at the region of the lesion. (**A**) TLS across cisPt-GG is more mutagenic in the G2 phase than in the G1 phase or S phase in MEF (gray bars) or U2OS cells (dark bars). (**B**) The overall mutagenicity of TLS across TT 6-4PP is similar in the various cell cycle phases (dark bars), but the mutagenic signature was different. For example, the prevalence of the hotspot mutation AAC→AAA (gray bars) in G2 is higher than in G1 or S. (**C**) The overall mutagenicity of TLS across BP-G is similar in the various cell cycle phases (dark bars), but the mutagenic signature is different. For example, the prevalence of the C→A mutation (gray bars) opposite BP-G in G2 was higher than in G1 or S. The detailed numerical results are presented in Supplementary Tables S3 and S4. *, statistically significant measurements. *P*-values are presented in the text.

relative contribution of each of these tolerance pathways is not precisely known due to the scarcity of appropriate assays. In mammals, TLS appears to play a major role in filling in of replication gaps caused by UV lesions as indicated by the severe phenotype of xeroderma pigmentosum variant patients who lack the TLS polymerase η (3), and by the essentiality in mice of Rev3L, the protein encoding the catalytic subunit of DNA polymerase ζ, a key TLS polymerase (41). In addition, studies performed in UV-irradiated mouse cells suggest that TLS is the dominant mechanism for filling-in these post-replication DNA gaps (18). Thus, the disappearance of the RPA foci in G2 is consistent with the operation of TLS to fill in these gaps.

The activity of TLS is determined by *cis*-acting DNA elements, e.g. the gaps formed in damaged DNA, as well as *trans*-acting factors, i.e. TLS proteins. Using the gapped plasmid TLS assay system enabled us to probe the cellular composition of the TLS machinery at the various cell cycle stages, since this assay monitors the operation of *trans*-acting factors on the plasmid. The results presented above, clearly indicate that the components of the TLS machinery change throughout the cell cycle, and exhibit their greatest activity during S and G2. The essence of these changes is unknown yet, but they do not seem to involve changes in the expression levels of the TLS polymerases η, ι and Rev1. In addition, there seemed to be no significant change in the ubiquitination of PCNA, which functions to recruit TLS polymerases to damaged sites in the DNA. Other possible regulatory mechanisms such as subcellular localization, post-translational modifications or the involvement of other regulatory proteins have not been addressed yet. The TLS machinery appears to remain functional also in the G1 phase, although we cannot rule out the possibility that some of this TLS occurs in the small fraction of early S phase cells that may be present in the G1 cells preparation. The existence of the TLS machinery in G1 is not particularly surprising, as it may function to fill in gaps that were formed by opposite lesions, e.g. by incidental strand displacement and excision reactions, or during the first step of interstrand crosslink repair. In addition, the TLS enzyme DNA polymerase κ was reported to function also in nucleotide excision repair, which operates in G1 (42). This is consistent with the presence of Ub-PCNA during G1 in UV-irradiated cells.

Interestingly, the mutagenic signature of TLS varied during the cell cycle. Notably, TLS across cisPt-GG was more mutagenic in G2 compared with S, both in human U2OS and MEF cells. TLS across TT 6-4PP and BP-G exhibited similar extent of mutagenicity in G2 and S; however, there were marked differences in mutagenic

specificity. Specifically, the AAC→AAA hallmark mutation at TT 6-4PP was more prevalent in G2 than in S, and the C→A transversion at BP-G was much more prevalent in G2 than in S. We have previously shown that Rev1 is required for the formation of the AAC→AAA hotspot mutation in mammalian cells (18), and therefore the large increase in the abundance of this mutation in G2 observed here is consistent with the action of Rev1 in post-replication gaps in G2. Taken together, these data support the notion that the composition of the TLS machinery changes along the cell cycle, which in some cases leads to more mutagenic TLS in G2. This may reflect an urgency in gap-filling as cells get close to mitosis, manifested by the activation of less accurate backup TLS pathways, and may explain the higher mutation rates observed at late replication times, when cells are closer to G2. This phenomenon was observed in both human (43) and *S. cerevisiae* cells (44) and in the latter, was shown to depend on TLS.

It could have been envisioned that lesions on the continuously synthesized leading strand arrest replication forks, whereas on the lagging strand, which is synthesized in a discontinuous manner, lesions cause the formation of gaps, because synthesis can reinitiate downstream of the lesion by a new Okazaki fragment. However, there is evidence from studies in *S. cerevisiae* (17) and *E. coli* (45,46) indicating that the presence of lesions can lead to gap formation on both the lagging and the leading strands, through replication reinitiation downstream of the lesions. Moreover, a recent study provided evidence for effective repriming past UV lesions during replication in human cells, leaving gaps opposite the lesions (47). Thus, one may envisage a situation in which the majority of replication discontinuities are gaps rather than arrested forks. When forks are arrested at lesions, relief of the block is likely to occur rather promptly, to prevent fork collapse and the formation of double-strand breaks, which are severe lesions. This implies that in such cases, lesion bypass would operate in the S phase. In contrast, there is less urgency in filling in replication gaps, the formation of which has little effect on replication fork progression in mammalian cells (18,47). Accordingly, TLS gap filling may start in S, but reaches its maximum in G2. In *S. cerevisiae*, a strongly increased expression of Rev1 (31) is likely to be involved in the higher TLS in G2. This is not the case in human cells, where the expression of Rev1 is not increased in G2 (Figure 3). Rev1 may still be involved by undergoing activation in G2, e.g. by post-translational modification, but other mechanisms may be involved as well.

At first glance, a strategy of postponing TLS up to late S and G2 appears to be a dangerous choice in mammalian cells, because that would mean having single-stranded regions exposed for a prolonged time, which increases the risk of producing highly deleterious double-strand breaks. Yet, the data presented here does indicate that TLS lags behind replication, and finishes its operation in G2 (Figure 6). We suggest that this mechanism ensures that chromosomal replication, which is an immense task, continues its operation with minimal delay, leaving behind the 'road repair work' of local patching of gaps. This gap repair can continue during G2, but apparently must be completed before the cell enters mitosis. The in-depth analysis of this mechanism may help to elucidate the involvement of TLS, and in particular, that of mutagenic TLS, in pathogenic processes, primarily carcinogenesis, where the formation of mutations plays a critical role.

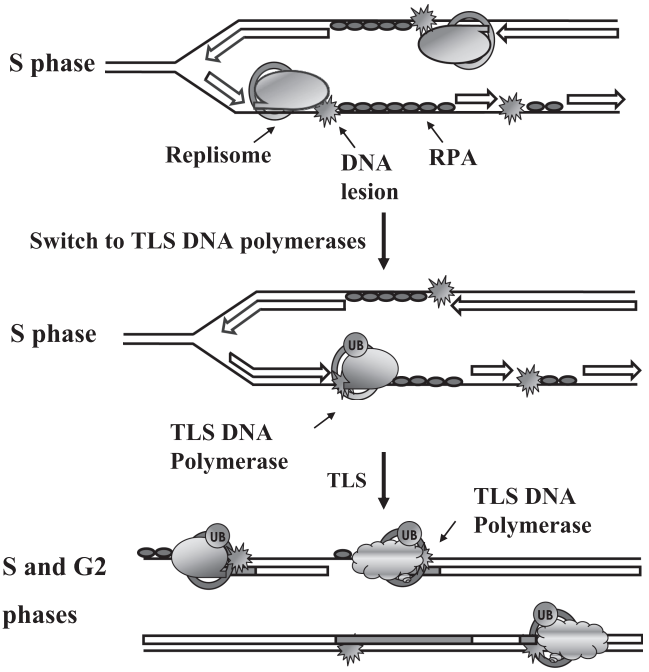

Figure 6. Model describing the activity of TLS in the S and G2 phases of the cell cycle. Lesions that have escaped excision repair cause a replication block. Upon stalling the replicative polymerase dissociates from the DNA, however, re-priming downstream to the lesion allows replication to continue, leaving behind the fork ssDNA regions bound to RPA. Monoubiquitination of PCNA initiates the recruitment of TLS polymerases to the gap during S phase. When the cells enter late S and G2 TLS becomes more robust (and sometimes more mutagenic) completing the filling-in of the gaps prior to mitosis.

SUPPLEMENTARY DATA

Supplementary Data are available at NAR Online.

ACKNOWLEDGEMENTS

We thank Poltoratsky V. and Wilson S.H. (NIEHS, USA) for a generous gift of anti-Rev1 antibodies, Jackson S.P. and Jazayeri A. (Cambridge University, Cambridge, UK) for advice on RPA staining, and Kiss V. (Weizmann Institute of Science, Rehovot, Israel) for his help with the microscopy experiments. Z.L. holds the Maxwell Ellis Professorial Chair in Biomedical Research.

FUNDING

Funding for open access charge: The Flight Attendant Medical Research Institute, Florida, USA (to Z.L.). Funding for the research: The Flight Attendant Medical Research Institute, Florida, USA (to Z.L.); Israel Science Foundation Grant 1136/08 (to Z.L.); U.S.

National Institutes of Health/National Cancer Institute grant CA099194 (to N.G.).

Conflict of interest statement. None declared.

REFERENCES

1. Prakash,S., Johnson,R.E. and Prakash,L. (2005) Eukaryotic translesion synthesis DNA polymerases: specificity of structure and function. *Annu. Rev. Biochem.*, **74**, 317–353.
2. Livneh,Z., Ziv,O. and Shachar,S. (2010) Multiple two-polymerase mechanisms in mammalian translesion DNA synthesis. *Cell Cycle*, **9**, 729–735.
3. Friedberg,E.C., Walker,G.C., Siede,W., Wood,R.D., Schultz,R.A. and Ellenberger,T. (2006) *DNA Repair and Mutagenesis*, 2nd edn. ASM Press, WA.
4. Yang,W. and Woodgate,R. (2007) What a difference a decade makes: Insights into translesion synthesis. *Proc. Natl Acad. Sci. USA*, **104**, 15591–15598.
5. Masutani,C., Kusumoto,R., Yamada,A., Dohmae,N., Yokoi,M., Yuasa,M., Araki,M., Iwai,S., Takio,K. and Hanaoka,F. (1999) The XPV (xeroderma pigmentosum variant) gene encodes human DNA polymerase eta. *Nature*, **399**, 700–704.
6. Johnson,R.E., Kondratick,C.M., Prakash,S. and Prakash,L. (1999) hRAD30 mutations in the variant form of xeroderma pigmentosum. *Science*, **285**, 263–265.
7. Ohmori,H., Friedberg,E.C., Fuchs,R.P.P., Goodman,M.F., Hanaoka,F., Hinkle,D., Kunkel,T.A., Lawrence,C.W., Livneh,Z., Nohmi,T. *et al.* (2001) The Y-family of DNA polymerases. *Mol. Cell*, **8**, 7–8.
8. Shachar,S., Ziv,O., Avkin,S., Adar,S., Wittschieben,J., Reissner,T., Chaney,S., Friedberg,E.C., Wang,Z., Carell,T. *et al.* (2009) Two-polymerase mechanisms dictate error-free and error-prone translesion DNA synthesis in mammals. *EMBO J*, **28**, 383–393.
9. Johnson,R.E., Washington,M.T., Haracska,L., Prakash,S. and Prakash,L. (2000) Eukaryotic polymerases ι and ζ act sequentially to bypass DNA lesions. *Nature*, **406**, 1015–1019.
10. Yoon,J.H., Prakash,L. and Prakash,S. (2009) Highly error-free role of DNA polymerase eta in the replicative bypass of UV-induced pyrimidine dimers in mouse and human cells. *Proc. Natl Acad. Sci. USA*, **106**, 18219–18224.
11. Hoege,C., Pfander,B., Moldovan,G.L., Pyrowolakis,G. and Jentsch,S. (2002) RAD6-dependent DNA repair is linked to modification of PCNA by ubiquitin and SUMO. *Nature*, **419**, 135–141.
12. Stelter,P. and Ulrich,H.D. (2003) Control of spontaneous and damage-induced mutagenesis by SUMO and ubiquitin conjugation. *Nature*, **425**, 188–191.
13. Kannouche,P.L., Wing,J. and Lehmann,A.R. (2004) Interaction of human DNA polymerase eta with monoubiquitinated PCNA: a possible mechanism for the polymerase switch in response to DNA damage. *Mol. Cell*, **14**, 491–500.
14. Avkin,S., Sevilya,Z., Toube,L., Geacintov,N.E., Chaney,S.G., Oren,M. and Livneh,Z. (2006) p53 and p21 regulate error-prone DNA repair to yield a lower mutation load. *Mol. Cell*, **22**, 407–413.
15. Friedberg,E.C., Lehmann,A.R. and Fuchs,R.P. (2005) Trading places: how do DNA polymerases switch during translesion DNA synthesis? *Mol. Cell*, **18**, 499–505.
16. Rupp,W.D. and Howard-Flanders,P. (1968) Discontinuities in the DNA synthesized in an excision-defective strain of *Escherichia coli* following ultraviolet irradiation. *J. Mol. Biol.*, **31**, 291–304.
17. Lopes,M., Foiani,M. and Sogo,J.M. (2006) Multiple mechanisms control chromosome integrity after replication fork uncoupling and restart at irreparable UV lesions. *Mol. Cell*, **21**, 15–27.
18. Jansen,J.G., Tsaalbi-Shtylik,A., Hendriks,G., Gali,H., Hendel,A., Johansson,F., Erixon,K., Livneh,Z., Mullenders,L.H., Haracska,L. *et al.* (2009) Separate domains of Rev1 mediate two modes of DNA damage bypass in mammalian cells. *Mol. Cell. Biol.*, **29**, 3113–3123.
19. Torres-Ramos,C.A., Prakash,S. and Prakash,L. (2002) Requirement of RAD5 and MMS2 for postreplication repair of UV-damaged DNA in Saccharomyces cerevisiae. *Mol. Cell. Biol.*, **22**, 2419–2426.
20. Karras,G.I. and Jentsch,S. (2010) The RAD6 DNA damage tolerance pathway operates uncoupled from the replication fork and is functional beyond S phase. *Cell*, **141**, 255–267.
21. Daigaku,Y., Davies,A.A. and Ulrich,H.D. (2010) Ubiquitin-dependent DNA damage bypass is separable from genome replication. *Nature*, **465**, 951–955.
22. Avkin,S., Goldsmith,M., Velasco-Miguel,S., Geacintov,N., Friedberg,E.C. and Livneh,Z. (2004) Quantitative analysis of translesion DNA synthesis across a benzo[*a*]pyrene-guanine adduct in mammalian cells. The Role of DNA polymerase *k*. *J. Biol. Chem.*, **279**, 53298–53305.
23. Poltoratsky,V., Horton,J.K., Prasad,R. and Wilson,S.H. (2005) REV1 mediated mutagenesis in base excision repair deficient mouse fibroblast. *DNA Repair*, **4**, 1182–1188.
24. Dart,D.A., Adams,K.E., Akerman,I. and Lakin,N.D. (2004) Recruitment of the cell cycle checkpoint kinase ATR to chromatin during S-phase. *J. Biol. Chem.*, **279**, 16433–16440.
25. Lehmann,A.R. and Fuchs,R.P. (2006) Gaps and forks in DNA Replication: Rediscovering old models. *DNA Repair*, **5**, 1595–1498.
26. Jazayeri,A., Falck,J., Lukas,C., Bartek,J., Smith,G.C., Lukas,J. and Jackson,S.P. (2006) ATM- and cell cycle-dependent regulation of ATR in response to DNA double-strand breaks. *Nat. Cell Biol.*, **8**, 37–45.
27. Richard,D.J., Bolderson,E. and Khanna,K.K. (2009) Multiple human single-stranded DNA binding proteins function in genome maintenance: structural, biochemical and functional analysis. *Crit. Rev. Biochem. Mol. Biol.*, **44**, 98–116.
28. Boutros,R. and Ducommun,B. (2008) Asymmetric localization of the CDC25B phosphatase to the mother centrosome during interphase. *Cell Cycle*, **7**, 401–406.
29. Jansen,J.G., Tsaalbi-Shtylik,A., Hendriks,G., Verspuy,J., Gali,H., Haracska,L. and de Wind,N. (2009) Mammalian polymerase zeta is essential for post-replication repair of UV-induced DNA lesions. *DNA Repair*, **8**, 1444–1451.
30. Guo,C., Fischhaber,P.L., Luk-Paszyc,M.J., Masuda,Y., Zhou,J., Kamiya,K., Kisker,C. and Friedberg,E.C. (2003) Mouse Rev1 protein interacts with multiple DNA polymerases involved in translesion DNA synthesis. *EMBO J.*, **22**, 6621–6630.
31. Waters,L.S. and Walker,G.C. (2006) The critical mutagenic translesion DNA polymerase Rev1 is highly expressed during G(2)/M phase rather than S phase. *Proc. Natl Acad. Sci. USA*, **103**, 8971–8976.
32. Moldovan,G.L., Pfander,B. and Jentsch,S. (2007) PCNA, the maestro of the replication fork. *Cell*, **129**, 665–679.
33. Ziv,O., Geacintov,N., Nakajima,S., Yasui,A. and Livneh,Z. (2009) DNA polymerase zeta cooperates with polymerases kappa and iota in translesion DNA synthesis across pyrimidine photodimers in cells from XPV patients. *Proc. Natl Acad. Sci. USA*, **106**, 11552–11557.
34. Hendel,A., Ziv,O., Gueranger,Q., Geacintov,N. and Livneh,Z. (2008) Reduced fidelity and increased efficiency of translesion DNA synthesis across a TT cyclobutane pyrimidine dimer, but not a TT 6-4 photoproduct, in human cells lacking DNA polymerase eta. *DNA Repair*, **7**, 1636–1646.
35. Gentil,A., Le Page,F., Margot,A., Lawrence,C.W., Borden,A. and Sarasin,A. (1996) Mutagenicity of a unique thymine-thymine dimer or thymine-thymine pyrimidine pyrimidone (6-4) photoproduct in mammalian cells. *Nucleic Acids Res.*, **24**, 1837–1840.
36. Berdichevsky,A., Izhar,L. and Livneh,Z. (2002) Error-free recombinational repair predominates over mutagenic translesion replication in E. coli. *Mol. Cell*, **10**, 917–924.
37. Izhar,L., Goldsmith,M., Dahan,R., Geacintov,N., Lloyd,R.G. and Livneh,Z. (2008) Analysis of strand transfer and template switching mechanisms in Escherichia coli: Predominance of strand transfer. *J. Mol. Biol.*, **381**, 803–809.
38. Adar,S., Hendel,A., Geacintov,N. and Livneh,Z. (2009) Repair of gaps opposite lesions by homologous recombination in mammalian cells. *Nucleic Acids Res.*, **37**, 5737–5748.
39. Branzei,D. and Foiani,M. (2010) Maintaining genome stability at the replication fork. *Nat. Rev. Mol. Cell. Biol.*, **11**, 208–219.

40. Zhang,H. and Lawrence,C.W. (2005) The error-free component of the RAD6/RAD18 DNA damage tolerance pathway of budding yeast employs sister-strand recombination. *Proc. Natl Acad. Sci. USA*, **102**, 15954–15959.
41. Gan,G.N., Wittschieben,J.P., Wittschieben,B.O. and Wood,R.D. (2008) DNA polymerase zeta (pol zeta) in higher eukaryotes. *Cell Res.*, **18**, 174–183.
42. Ogi,T., Limsirichaikul,S., Overmeer,R.M., Volker,M., Takenaka,K., Cloney,R., Nakazawa,Y., Niimi,A., Miki,Y., Jaspers,N.G. *et al.* (2010) Three DNA polymerases, recruited by different mechanisms, carry out NER repair synthesis in human cells. *Mol. Cell*, **37**, 714–727.
43. Stamatoyannopoulos,J.A., Adzhubei,I., Thurman,R.E., Kryukov,G.V., Mirkin,S.M. and Sunyaev,S.R. (2009) Human mutation rate associated with DNA replication timing. *Nat. Genet.*, **41**, 393–395.
44. Lang,G.I. and Murray,A.W. (2011) Mutation rates across budding yeast Chromosome VI are correlated with replication timing. *Genome Biol. Evol.*, Epub ahead of print, doi:10.1093/gbe/evr054.
45. Heller,R.C. and Marians,K.J. (2006) Replication fork reactivation downstream of a blocked nascent leading strand. *Nature*, **439**, 557–562.
46. Langston,L.D. and O'Donnell,M. (2006) DNA replication: keep moving and don't mind the gap. *Mol. Cell*, **23**, 155–160.
47. Elvers,I., Johansson,F., Groth,P., Erixon,K. and Helleday,T. (2011) UV stalled replication forks restart by re-priming in human fibroblasts. *Nucleic Acids Res.*, **39**, 1360–1371.